Title
HEAVY-ION PROJECTILES AND IN-BEAM SPECTROSCOPY

Authors
Diamond, R.M.
Stephens, P.S.

Publication Date
1966-09-01

UCRL-17143

University of California

Ernest O. Lawrence Radiation Laboratory

HEAVY-ION PROJECTILES AND IN-BEAM SPECTROSCOPY

Berkeley, California

DISCLAIMER

Submitted to Arkiv Physik

UCRL-17143
Preprint

UNIVERSITY OF CALIFORNIA

Lawrence Radiation Laboratory
Berkeley, California

AEC Contract No. W-7405-eng-48

HEAVY-ION PROJECTILES AND IN-BEAM SPECTROSCOPY

R.M. Diamond and F.S. Stephens

September 1966

International Symposium on "Why and How Should We Investigate Nuclides Far Off The Stability Line?" Lysekil, Sweden August 21-27, 1966

HEAVY-ION PROJECTILES AND IN-BEAM SPECTROSCOPY

R.M. Diamond and F.S. Stephens

Lawrence Radiation Laboratory
University of California
Berkeley, California

September 21, 1966

In-beam spectroscopy, though sometimes involving technical problems not faced by more conventional nuclear spectroscopy, allows the study of a wide range of nuclei, including, in principle, all the β-stable and (bound) neutron-deficient species. A special advantage of this wide range is that a series of related nuclei can be populated in a uniform way, enabling one to study the systematics of the level(s) of interest. For such in-beam studies (and for some out-of-beam purposes, also) the use of heavy ions as bombarding projectiles offers certain advantages. We would like to mention and illustrate four: 1) high nuclear charge; 2) large linear momentum transfer; 3) high nuclear product specificity; 4) large angular momentum transfer.

I. HIGH NUCLEAR CHARGE.

Heavy-ion projectiles play a very important, almost dominant, role in present-day Coulomb excitation studies, and since the reason is well-known, only brief mention is given here. Coulomb excitation has the advantage over other nuclear reactions that the process is understood and the theory is well developed.[1,2] Thus in particular, the reduced transition probabilities between the ground state and excited states which are important in evaluating nuclear models, are readily and reliably determined in this manner. With protons as projectiles, essentially only the first excited state can be reached in even-even nuclei and only the first two or few states in odd-mass ones. This is because the probability of exciting a state falls off with increasing level energy, and because multipole excitations other than E2 are, for various reasons, usually difficult to observe. But with heavy-ion projectiles the electric field exerted at the target nucleus goes up, and so does the probability of excitation. For the strong collective E2 transitions these probabilities became appreciable, so that multiple Coulomb excitation becomes increasingly important. Figure 1 shows the increased number of transitions found with multiple Coulomb excitation of ^{232}Th on going from 70 MeV ^{16}O to 190 MeV ^{40}Ar. Figures 2 and 3 give the energy levels found by multiple Coulomb excitation of ^{238}U, including the ground-state rotational band through the I=14 member. Values of the excitation B(Eλ)'s to the vibrational bands and of branching ratios of the gamma transitions to the ground-state band are also obtained.[3]

Double E2 Coulomb excitation was first observed in tungsten with ^{16}O ions only eight years ago,[4] but by now multiple excitation with heavy ions has been used in too many studies to be catalogued here.[5] However, measurement of certain special higher order effects now come within the realm of possibility.

An example is the reorientation effect[6] where one of the steps in the excitation is from one magnetic substate to another in the same level. This process occurs through the interaction of the projectile with the quadrupole moment of the excited state, and depends linearly on the moment, yielding not only its magnitude but also its sign. The first such determination of an excited state quadrupole moment was obtained by deBoer, Stokstad, Symons, and Winther[7] by finding a 10% difference in the ratio of the experimental yield of the first excited 2+ state in ^{114}Cd to that calculated by first order theory when using ^{4}He and ^{16}O ions as projectiles. The large value of Q_{2+} necessary to account for this difference, $Q_{2+} = (-0.70 \pm 0.21) \times 10^{-24}$ cm^2, shows that this nucleus, considered spherical in its ground state, is deformed in the 557.8 keV 2+ level, and is another indication that the harmonic oscillator is an unsatisfactory model for such nuclei.

II. LARGE LINEAR MOMENTUM TRANSFER.

Conservation of linear momentum permits, if thin targets are used, a rather narrow angular cone of recoiling nuclei of relatively large and uniform velocity ($v/c \approx 1$-10%) to be obtained in heavy-ion reactions. This may be desirable for a number of uses. One is simply as a means of quickly separating the product nuclei from the target. This is important if one desires to examine the radiation from short-lived nuclei and the target material is radioactive, as is the case in the study of the transcurium isotopes. One of the first such uses[8] was in the production of ^{248}Fm and of ^{254}102 by 60-100 Mev ^{12}C irradiation of ^{240}Pu and of ^{244}Cm. The recoiling, positively-charged nuclei were slowed in the gas and then attracted to a moving negatively-

charged metallic belt placed beneath the target. This belt carried them under a foil, charged still more negatively, which captured about 1/2 of the daughter nuclei recoiling away from the belt after α-decay of the parent atoms. In this way the daughter nuclei could be studied quite free of the target activity, and the half-life of the parent could be determined by varying the position of the foil and the speed of the belt.

Or, the recoil can be used to transfer the product nuclei quickly into an environment suitable for various measurements. One example might be as a means of introducing the reaction products directly and rapidly into an on-line mass separator; this will possibly become an important technique in the future. Another example is the recoil implantation of Coulomb excited nuclei into ferromagnetic backing so as to measure, by the method of perturbed angular correlation, the magnetic moments of excited states or the internal fields at the impurity nucleus in the host material. As done by the Copenhagen groups[9,10,11] Coulomb excited nuclei recoil out of a thin ($\sim$100 ug/cm^2) target into an iron-foil backing which is magnetized by a small external field. A ring counter accepts the heavy ions scattered at some back angle, and is in coincidence with movable NaI counters which measure the angular distribution of the de-exciting gamma rays with respect to the beam direction. Since the recoiling nuclei are stopped in the iron in $\sim 10^{-13}$ sec, their alignment will not be significantly disturbed by the stopping process. By analyzing the shift of the correlation caused by the internal field in the iron foil, one can obtain the product of the Larmor velocity and the mean life of the level, $\omega\tau$, and knowing τ this yields $\omega = -gH\mu_n/\hbar$. If the effective field at the nucleus, H, is known, the value of g for the excited state is determined, or conversely, knowing or estimating g, the internal magnetic field at the

impurity nuclei can be determined.

The large recoil velocities obtained with heavy ions are useful in the measurement of very short lifetimes of excited states produced in the reaction. Reviews on the subject should be consulted for details[12]; we shall only mention briefly three recent applications.

In the direct-distance-measurement method, the number of gamma rays or conversion electrons observed at right angles to the beam axis per fixed number of reactions is determined as a function of distance from the target to the detector defining slits, that is, as a function of the distance the recoils travel before decay. If all recoiling nuclei have the same velocity and direction, the product $v\tau$ is readily determined. Since distances down to 10^{-3} cm can be measured, $v\tau \geq 10^{-3}$ cm, and for recoil velocities of 10^{8} cm/sec, $\tau \geq 10^{-11}$ sec. But with the order-of-magnitude larger velocities imparted by heavy ions, a 10 times shorter half-life may be measured. A modification using Doppler-shifted gamma rays has been performed by Wright,[13] and improved still further by Alexander and Allen[14] with the use of a lithium-drifted Ge counter. In the latter group's experiment, the Doppler-shifted gamma-ray peak, $E = E_0(1 + \frac{v}{c} \cos \theta)$, from nuclei recoiling in vacuo from the target can be separated by the Ge counter from the unshifted gamma rays, of energy E_0, from nuclei stopped in a metal plunger near the target. By determining the ratio of the intensity of the unshifted gamma-ray peak to the total number of decays (recorded with a NaI monitor counter, for example) as a function of distance of the plunger from the target, $v\tau$ is obtained. And the value of the average recoil velocity, v, is given by the direct observation of the Doppler shift at the fixed angle of the Ge counter. By this means they were able to determine mean lifetimes of $(2.33 \pm 0.27) \times 10^{-10}$ and

$(2.5\pm0.2) \times 10^{-11}$ sec for the 0.871 and 6.13 MeV states in ^{17}O and ^{16}O, respectively.

For still shorter lifetimes, from 10^{-11} to 10^{-14} sec, the Doppler-shift attenuation method is applicable. In this technique the nuclei recoil into a backing with a known "slowing down time", e.g., 9×10^{-13} sec for Mg and 3.5×10^{-13} sec for Cu. If part of the nuclei emit their gamma rays before stopping, the half-life is comparable to the slowing down time; if only Doppler-shifted gamma rays are observed, it is shorter; and if only unshifted gamma rays are seen, it is larger. Actual measurement of the fraction of the total Doppler shift observed with different backings yields a quantitative measure of the nuclear lifetime if the rate of energy loss of the nuclei in the stopping material is known or can be estimated. Litherland, Yates, Hinds, and Eccleshall give a good example of this method using ^{16}O as projectiles.[15]

We would also like to mention a recoil-distance measuring technique we have used.[16] It is a modification of a method devised by Novakov, Hollander, and Graham,[17] using the recoil from α-decay of a heavy element and a high resolution iron-free electron spectrometer. With the larger recoil velocities obtained in heavy-ion reactions, we were able to get by with a small wedge-gap spectrometer. Figure 4 shows the scheme of the target arrangement. Conversion electrons from the recoiling nuclei are given off before the nuclei reach the negative high voltage grid (placed at a distance depending on the lifetime of the level). The electrons are then slowed down by the negative-voltage gradient an amount depending on their distance of emission from the grid. After passing the grid, the electrons are accelerated through the full voltage gradient. In this manner an electron is given an additional amount of

energy, the magnitude of which depends on the recoil distance before electron emission, and therefore on the lifetime of the nuclear state involved. By applying the high voltage only during every other Hilac beam pulse, a perturbed and an unperturbed conversion electron peak could be recorded during the same spectrometer magnet sweep. Knowing the applied voltage, the distance from target to first grid, and the recoil velocity, the lifetime can be determined from the exponential slope on the high energy side of the electron peak, or from the shift in the peak position with voltage on and off. An example of the spectrum obtained for the first-excited 2+ state in ^{126}Ba made by 52 MeV ^{14}N on ^{115}In is shown in Fig. 5; the mean lifetime determined is $2.7 \pm 0.5 \times 10^{-10}$ sec.

III. HIGH NUCLEAR PRODUCT SPECIFICITY

There are a variety of ways of producing a particular neutron-deficient nucleus. One way is to irradiate a stable isotope one (two) lower in atomic number than the desired nucleus with protons (alphas) of sufficient energy to boil off enough neutrons to reach the intended product. This has a drawback in that all the heavier isotopes that can be made will be made at the same time, due to the long, high-energy tails on the excitation functions for these xn reactions. The resulting mixture of activities must be used as is, being sorted out by the different half-lives, or it must be mass-separated. However, by proper choice of the target nucleus and projectile, the number of activities in the mixture can be minimized. A reaction is chosen to make the product such that it is the first (HI,xn) reaction to occur with significant yield above the Coulomb barrier for that particular projectile-target pair. Consider, for example, the production of ^{193}Tl. It can be made by ^{197}Au(^{4}He,8n)^{193}Tl or by ^{181}Ta(^{16}O,4n)^{193}Tl; the latter reaction occurs just above the barrier. Germanium counter gamma-ray spectra taken in-beam

show transitions in heavier thallium nuclei in the first case, but not in the second.

IV. LARGE ANGULAR MOMENTUM TRANSFER

In a typical compound nucleus reaction of 80-90 MeV ^{11}B ions on a target of mass 150-200, from a few up to 50 or more units of angular momentum may be transferred, according to a simple classical calculation. For heavier or higher-energy projectiles, the maximum will be still higher. Actually, the maximum is not so high as calculated classically because most of the collisions at the surface of the nucleus, which would give the largest values, do not produce compound nuclei but go into direct reactions, nuclear transfer, pick-up and stripping. But still, the mean value of the momentum transferred can be large. Subsequent emission of a few neutrons does not change the picture appreciably, as they carry off little momentum, $1/2\hbar$-$2\hbar$ apiece. Typically the neutron emission lowers the excitation energy to a few MeV, and a gamma-ray cascade completes the deexcitation. Because of the large amount of angular momentum to be removed, and the relatively low excitation energy, a predominantly stretched cascade of gamma radiation may occur, and quadrupole transitions might be favored. Such a gamma-ray cascade may even start above the last neutron binding energy; neutron emission, although energetically possible, may not readily occur because there is no suitable high-spin state in the residual nucleus some 8-10 MeV lower in excitation energy, and the centrifugal barrier hinders the emission of particles with large orbital momentum. Grover[18,19] has shown that such gamma-ray competition with neutron emission does occur, particularly in reactions involving ^{4}He or heavier projectiles, and that it helps explain the inconsistency in determinations of the level density parameter, a, by excitation function measurements and

by particle spectra, and the apparently too copious gamma-ray production in heavy-ion reactions. A fundamental rule of compound nucleus formation, that the modes of formation and decay are independent, is violated by the conservation of angular momentum; the excited nucleus has a link to how it was formed through its angular momentum distribution.

In any case, we are interested in observing the de-excitation gamma-ray cascade; with a deformed even-even nucleus one might expect to see the ground-state rotational band, to high spin values and perhaps the rotational bands built on the first β- and γ- vibrational states. And in spherical nuclei one might expect to see the high-spin members of the vibrational multiplets.

Such de-excitation cascades have been studied by Morinaga and Gugelot in $(\alpha,4n)$ reactions[20] and by Hansen, Elbek, Hagemann, and Hornyak in $(p,2n)$ reactions.[21] We have used (HI,xn) reactions where HI ranged from ^{4}He to ^{19}F, and have observed the conversion electrons and/or gamma rays in the final cascade for some 25 reactions.[16,22,23] Figure 6 shows two typical conversion electron spectra for even-even deformed nuclei. We have studied about a dozen such cases, and observe the ground-state rotational band up to spin 14, sometimes 16, and in two or three cases to 18. The results of these studies can be summarized in the following observations: 1) only ground-state band transitions are observed in significant intensity (no vibrational band transitions); 2) the rotational transition energies fall increasingly below those of the rigid rotor

$$E_I - E_{I-2} = \hbar^2(4I-2)/2\Im$$

as I increases; 3) the transition energies for the different nuclei become

increasingly similar at large I. These last two points are more graphically illustrated in Fig. 7 where $A_I = \hbar^2/2\Im$ is plotted vs I. Under rotation these different nuclei appear to achieve a more common set of properties. We think they may all stretch out under the centrifugal force against a restoring potential which becomes more similar at larger deformation as the shell effects are washed out, and liquid drop characteristics are more nearly approached.[24]

As one goes up in atomic number from the rare earth region of deformed nuclei to the spherical nuclei below lead, the final gamma-ray cascade changes in nature, as shown in Figs. 8, 9, and 10. The rotational sequence observed changes to a quasi-rotational cascade and then to the highest spin member of the vibrational multiplets.[23] The spectra appear to become more complex at first, with extraneous transitions other than the stretched quasi-rotational cascade appearing, sometimes of multipolarity different from E2, e.g., the 623 keV E2 in ^{178}Os, and the 412 keV M1, 417 keV E2, 582 keV E1, 892 keV E1 in ^{188}Pt. And with the spherical nuclei, the cascade is seen only up to spins 6 or 8, much lower values than with the deformed nuclei. We do not know the reasons for this, as approximately the same (large) amount of angular momentum has been brought into the compound nucleus, but we offer the following speculation. With the spherical nuclei, the level spacing is large, ~400 KeV, and so the level of spin 6 is already at ~1.5 MeV, near the pairing gap. We know that two-quasi-particle states can exist above the gap with spins as high as 8 or 10 (we have observed $I\pi = 8^-$, K=8, isomers in ^{182}Os and ^{184}Pt). Thus, above the gap there are probably many paths down from the initial spin distribution of up to 30 or so; the intensity is distributed among these paths so that they cannot be distinguished individually but contribute to a continuum of gamma rays going up to several MeV in energy. Only below the gap is there a unique path down in spin to the ground state, and so enough intensity in the individual

transitions for them to be seen.

We may add these more spherical nuclei to the plot of Fig. 7 of A_I vs I. This is done in Fig. 11 where the three small circles at I=8, 12 and 16 indicate the common curve reached by the deformed nuclei. Some points have been included for ^{200}Hg, ^{196,190}Pt, and ^{190,186}Os from data in the literature. It can be seen that six of the new group of nuclei approach the previous common curve at high spin, even though their initial $2 \rightarrow 0$ transition energies are higher than for the better deformed nuclei. We believe this means that even though they may be little deformed initially, they are very soft towards deformation along the symmetry axis, and so, under rotation, they stretch rapidly out to the shape of the originally more highly deformed, but more rigid, nuclei.

But clearly there is a gradual change in behavior in going to the heavy osmium nuclei. The latter do not come down to the common curve, at least by the spins observed. It is known that in just these nuclei the gamma-vibrational band drops with increasing mass number from above 1 MeV to become the second excited state in ^{192}Os at 489 keV, and we believe these two features are related. Nuclei with low-lying gamma-vibrational bands, have a more shallow potential-energy surface as a function of γ than do prolate deformed nuclei which have a distinct minimum along the β-axis, i.e., $\gamma = 0$. As a result they are soft towards non-axial, as well as axial, stretching, and the effects of non-axial deformation under rotation might be expected to yield a different behavior than deformation along the axis only. From Fig. 11 it can be seen that a similar change in the A_I vs I curve takes place more sharply between ^{186}Pt and ^{188}Pt, and we tentatively suggest that the γ-band becomes lower and its ground-state interaction becomes more important at this point. We might add that the addition of nuclei as different as ^{126}Ba, ^{122,120}Xe, ^{232}Th, and ^{238}U

to the plot of Fig. 11, after an empirical mass normalization of $A^{5/3}$ to A = 170 gives a continued grouping of the curves at high spin. The deformed ^{232}Th and ^{238}U nuclei behave very much like the deformed rare earths, and the barium and xenon isotopes behave like ^{184}Pt, little deformed initially but apparently stretching out rapidly to the same prolate shape as the others.

As a last topic, we would like to mention a new development that results from the large amount of angular momentum brought into compound nucleus formation by heavy-ion irradiation. It is well-known that this momentum contributes only to the m=0 substate, taking the beam direction as the axis. The resulting compound nuclei are highly aligned; the only deviation from a pure m=0 distribution comes from the initial spins of the target and projectile. The subsequent evaporation of 4-5 neutrons does not change this much, as the low-energy neutrons cannot carry off much angular momentum nor broaden the magnetic substate distribution much. So the nuclei remain in relatively high spin states and strongly aligned when starting the final gamma-ray cascade. Thus the gamma transitions should show an angular correlation with the direction, and since the ground state rotational band produces a stretched cascade of E2 transitions in going from the high spin states to the spin 0 ground state, the correlations will tend to be the same for all these gamma rays.

It has been shown by Ejiri, Ishihari, Sakai, Katori, and Inamura[25] that the conversion electrons emitted in the cascade following proton- and alpha-induced reactions are indeed anisotropic, and Williamson and Shepherd[26] have shown the same for the rotational gamma transitions following $(\alpha,3n)$ reactions in three rare earth nuclei. We have studied, using lithium-drifted Ge counters, the angular distributions of the gamma-ray cascades following 12-15 reactions induced by heavy ions (^{4}He to ^{19}F) and leading to deformed and spherical

even-even nuclei in the mass range 160-200.[27,28] Very marked angular distributions were observed. Figure 12 shows the 0° and 90° (reduced by 10) spectra in $^{172}_{72}Hf$. The spectra are similar, but the transition intensities at 0° are about 1-1/2 times larger than those at 90°. This is better seen in Fig. 13 where the angular distribution of the $6 \rightarrow 4$ transition is given along with the values of A_2 and A_4 in the distribution expression

$$W(\theta) = 1 + A_2 P_2(\cos\ \theta) + A_4 P_4(\cos\ \theta) + \ldots$$

The distributions for the other transitions are very similar, as are those for the other dozen even-even nuclei studied. The results are summarized in Fig. 14, where $-A_4$ is plotted against A_2 for all transitions other than the $2 \rightarrow 0$. The latter have been excluded since their distributions are partially attenuated by extranuclear effects.

Two conclusions can be reached. First, the experimental points are bunched; all fall within $A_2 = 0.30 \pm 0.09$ and $A_4 = -0.09 \pm 0.05$ (Fig. 14 shows only one of four possible quadrants). Second, the values of A_2 are large, and near the limiting value for complete m=0 alignment of the initial states, when they have $I \geq 20$; the latter limit is $A_2 = 0.38$, and $A_4 = -0.13$. The line in the figure gives the relationship between A_2 and A_4 expected for a Gaussian Distribution of magnetic substates centered around m = 0. For a not-too-broad distribution, this is a reasonably good representation of the distribution calculated to be obtained from an initially pure m=0 system after the emission of a few neutrons and/or gamma rays. Deviations from this curve would occur if there are unstretched transitions in the cascade, and if there is feeding from lower spin states with the same initial spread of magnetic substates.

Obviously the nuclei produced in these heavy-ion induced compound nucleus reactions are highly aligned and the gamma-ray cascade is predominantly a stretched cascade having a marked angular distribution. We feel that this will be a useful tool in nuclear spectroscopy studies, particularly of the odd-mass and odd-odd nuclei, and in studies of magnetic moments and hyperfine interactions of excited states. We would like to illustrate the first case with an example taken from an in-beam study of the levels of the neutron-deficient odd-mass thallium nuclei.[29] In the reaction $^{197}Au(^{4}He,2n)^{199}Tl$ we have found, among others, three gamma-ray transitions of 331, 370 and 701 keV which lie above the 749 keV, 9/2- isomeric state. From their energies and intensities, we believe they connect two higher levels with the isomeric state, as shown in the insert in Fig. 15. The three transitions have large angular distributions, as shown in the figure. With the reasonable assumption that they are dipole or quadrupole or mixed transitions, there are 19 possible spin sequences leading to the 9/2- level. From the signs and magnitudes of the experimental values of A_2, the number of spin sequences is unambiguously reduced to 5. Consideration of the expected alignment of the thallium nuclei by comparison with the even-even cases shown in Fig. 14 reduced this number to the three cases shown on the insert in Fig. 15. A measurement of the conversion coefficient of the 701 keV transition, showing it to be predominantly E2, rules out two of these (wrong sign for A_2), leaving only the sequence $13/2 \rightarrow 11/2 \rightarrow 9/2-$, a stretched cascade from higher to lower spin.

The E2/M1 mixing amplitude and its sign can also be determined for a mixed transition when the alignment of the initial state can be obtained or estimated. For example, the mixing amplitude of the 331 keV transition can be obtained, as it comes from a level (13/2-) whose magnetic substate distribution is given by

the angular distribution of the 701 keV transition (assumed pure E2). The ratio $A_2(13/2 \rightarrow 11/2)/A_2(13/2 \rightarrow 9/2)$ for the two transitions is thus equal to the ratio $F_2(1\ 1\ 11/2\ 13/2) + 2\delta F_2(1\ 2\ 11/2\ 13/2) + \delta^2 F_2(2\ 2\ 11/2\ 13/2)$ / $F_2(2\ 2\ 9/2\ 13/2)$ of known F-coefficients. A plot of $A_2(13/2 \rightarrow 11/2)$ vs δ (or %E2 or %M1) using the experimental value of $A_2(13/2 \rightarrow 9/2)$ yields an elliptical band which is cut in two regions by the experimental value of $A_2(13/2 \rightarrow 11/2)$, Fig. 16. A decision is possible between the two values by the similar crossing of the theoretical line for $A_4(13/2 \rightarrow 11/2)$ by the experimental one. In a similar way an estimate of δ for the 370 keV transition can be obtained by taking the alignment of its initial state as comparable to that of the corresponding level in the even-even examples given in Fig. 14. Clearly a large amount of useful information can be obtained in this case from the simple measurement of the angular distributions of these three transitions.

The high degree of nuclear alignment obtained in heavy-ion reactions should also be possible to use in the measurement of electromagnetic moments and hyperfine interactions of excited nuclear levels by the methods of perturbed angular correlations. The lower limit to the usable lifetimes is set by the minimum time to get appreciable precession of the nucleus in the effective field, and the upper limit by the relaxation time of the nucleus in the environment. In such studies, the large recoil velocity imparted the nucleus by heavy-ion irradiation is an aid in getting the nucleus into a suitable environment. For short-lived levels in the 10^{-11}-10^{-9} sec range, a ferro-magnetic backing would be useful so as to obtain a large effective magnetic field, as has already been used in the Coulomb excitation experiments described earlier. For half-lives in the 10^{-9}-10^{-3} sec range, the same ferromagnetic environment can be used for resonance destruction of the angular distribution.[30] For conventional spin-

rotation measurements in an external magnetic field, the recoiling nuclei should go into nonmagnetic cubic crystals to avoid, as far as possible, attenuating interactions.

Certainly the use of reaction-induced nuclear alignment will be an important technique in in-beam spectroscopy in the future, and in-beam spectroscopic studies appear a most promising and convenient way to study the nuclei far removed from stability on the neutron-deficient side.

Acknowledgements. This work was supported in part by the U.S. Atomic Energy Commission. One of the authors (R.M.D.) would like to thank the Tandem Accelerator Laboratory of the Niels Bohr Institute for the hospitality accorded him as a visiting Guggenheim fellow.

REFERENCES

1. K. Alder, A. Bohr, T. Huus, B. Mottelson, and A. Winther, Rev. Mod. Phys. 28, 432 (1956) and Refs. therein for earlier work.
2. K. Alder, and A. Winther, Mat. Fys. Medd. Dan. Vid. Selsk. 32, No. 8 (1960)
3. F.S. Stephens, B. Elbek, and R.M. Diamond, (to be published).
4. J.O. Newton, and F.S. Stephens, Phys. Rev. Letters 1, 63 (1958)
5. See, for example, Coulomb Excitation, Section E in "Proceedings of the Third Conference on Reactions between Complex Nuclei," ed. A. Ghiorso, R.M. Diamond, and H.E. Conzett, (Berkeley, University of California Press, (1963).
6. G. Breit, and J.P. Lazarus, Phys. Rev. 100, 942 (1955).
7. J. De Boer, R.G. Stokstad, G.D. Symons, and A. Winther, Phys. Rev. Letters 14, 564 (1965).
8. A. Ghiorso, T. Sikkeland, J.R. Walton, and G.T. Seaborg, Phys. Rev. Letters 1, 18 (1958).
9. L. Grodzins, R. Borchers, and G.B. Hagemann, Phys. Letters 21, 214 (1966).
10. F. Boehm, G.B. Hagemann, and A. Winther, Phys. Letters 21, 217 (1966)
11. F. Boehm, and G.B. Hagemann, Proc. Moscow Conf. Nucl. Spectr. Izv. Akad. Nauk. S.S.S.R. Ser. Fiz., (to be published).
12. S. Devons, The Measurement of Very Short Lifetimes, "Nuclear Spectroscopy, Part A," ed. F. Ajzenberg-Selove (New York, Academic Press, 1960) p.512. S. Devons, G. Manning, D.StP. Bunbury, Proc. Phys. Soc. (London) 68, 18 (1955)
13. I.F. Wright, Bull. Am. Phys. Soc. Series II, 6, 285 (1961).
14. T.K. Alexander, and K.W. Allen, Bull. Am. Phys. Soc. Series II, 10, 118 (1965).

15. A.E. Litherland, M.J.L. Yates, B.M. Hinds, and D. Eccleshall, Nucl. Phys. 44, 220 (1963).

16. J.E. Clarkson, PhD Thesis, 1965, University of California, Berkeley, California.

J.E. Clarkson, R.M. Diamond, F.S. Stephens, and I. Perlman, (to be published).

17. T. Novakov, J.M. Hollander, and R.L. Graham, Nucl. Instr. Methods 26, 189 (1964).

18. J.R. Grover, Phys. Rev. 123, 267 (1961); Phys. Rev. 127, 2142 (1962).

19. J.R. Grover, and R.J. Nagle, Phys. Rev. 134, B1248 (1964).

20. H. Morinaga, and P.C. Gugelot, Nucl. Phys. 46, 210 (1963).

21. G.B. Hansen, B. Elbek, K.A. Hagemann, and W.F. Hornyak, Nucl. Phys. 47, 529 (1963).

22. F.S. Stephens, N. Lark, R.M. Diamond, Phys. Rev. Letters 12, 225 (1964); Nucl. Phys. 63, 82 (1965).

23. J. Burde, R.M. Diamond, and F.S. Stephens, (to be published).

24. R.M. Diamond, F.S. Stephens, and W.J. Swiatecki, Phys. Letters 11, 315 (1964).

25. H. Ejiri, M. Ishihari, M. Sakai, K. Katori, and T. Inamura, Phys. Letters 18, 314 (1965).

26. C.F. Williamson, and B.J. Shepherd, Bull. Am. Phys. Soc. 10, 428 (1965).

27. R.M. Diamond, E. Matthias, J.O. Newton, and F.S. Stephens, Phys. Rev. Letters 16, 1205 (1966).

28. J.O. Newton, R.M. Diamond, K. Kotajima, E. Matthias, and F.S. Stephens, (to be published).

29. S. Cirilov, R.M. Diamond, J.O. Newton, and F.S. Stephens, (to be published).

30. E. Matthias, D.A. Shirley, M.P. Klein, and N. Edelstein, Phys. Rev. Letters 16, 974 (1966).

FIGURE CAPTIONS

1. Comparison of the Coulomb excitation spectra of ^{232}Th made with 70 MeV ^{16}O and 190 MeV ^{40}Ar. These are singles spectra taken with a lithium-drifted Ge counter.
2. Even-parity energy levels in ^{238}U. Transitions as observed in Coulomb excitation.
3. Odd-parity levels in ^{238}U. Transitions as observed in Coulomb excitation.
4. Schematic of lifetime measuring apparatus. The distance C could be varied between certain limits.
5. The K-electron line of the 256 keV 2 → 0 transition in ^{126}Ba from ^{115}In(^{14}N,3n)^{126}Ba, showing the effect of applying high voltage in the lifetime apparatus.
6. Conversion electron spectra in ^{166,164}Yb taken in-beam. The reactions are indicated.
7. Transition rotational constants for: ^{172,174,176}W, closed symbols; ^{166,168,170,172}Hf, open symbols; ^{166}Yb, half-closed symbols.
8. Conversion electron and gamma-ray (Ge counter) spectra in ^{178}Os from ^{169}Tm(^{14}N,5n)^{178}Os.
9. Conversion electron and gamma-ray (Ge counter) spectra in ^{188}Pt from ^{181}Ta(^{11}B, 4n)^{188}Pt.
10. Conversion electron and gamma-ray (G counter) spectra in ^{190}Hg from ^{181}Ta(^{14}N,5n)^{190}Hg.
11. Transition rotational constants for indicated nuclei vs I. Three small circles indicate average curve from Fig. 7.
12. Gamma-ray spectra, taken at 0° and 90° to the beam axis, in ^{172}Hf from ^{165}Ho(^{11}B,4n)^{172}Hf. Annihilation radiation peak (511 keV) comes

between the 10 → 8 and 12 → 10 transitions.

13. Angular distribution of the 319 KeV 6 → 4 transition in ^{172}Hf.

14. Plot of (the angular distribution coefficients) $-A_4$ vs A_2 for a number of rotational or vibrational gamma-ray transitions in even-even nuclei produced by heavy-ion (^{4}He-^{19}F) reactions. The line represents the relationship between $-A_4$ and A_2 expected for a Gaussian population of magnetic substates centered around m=0.

15. The observed angular distributions with respect to the beam direction of three gamma-rays in ^{199}Tl from $^{197}Au(^{4}He,2n)^{199}Tl$. The placement of these transitions above the 749 keV, 9/2- isomeric level in ^{199}Tl is shown in the insert along with the probable spins based on the angular distributions.

16. Plot of distribution coefficients, A_K, vs %M1 in the 331 keV, mixed M1-E2 transition in ^{199}Tl. The width of the theoretical bands comes from the experimental errors in the determinations of $A_K(13/2 \rightarrow 9/2)$ used in the calculation.

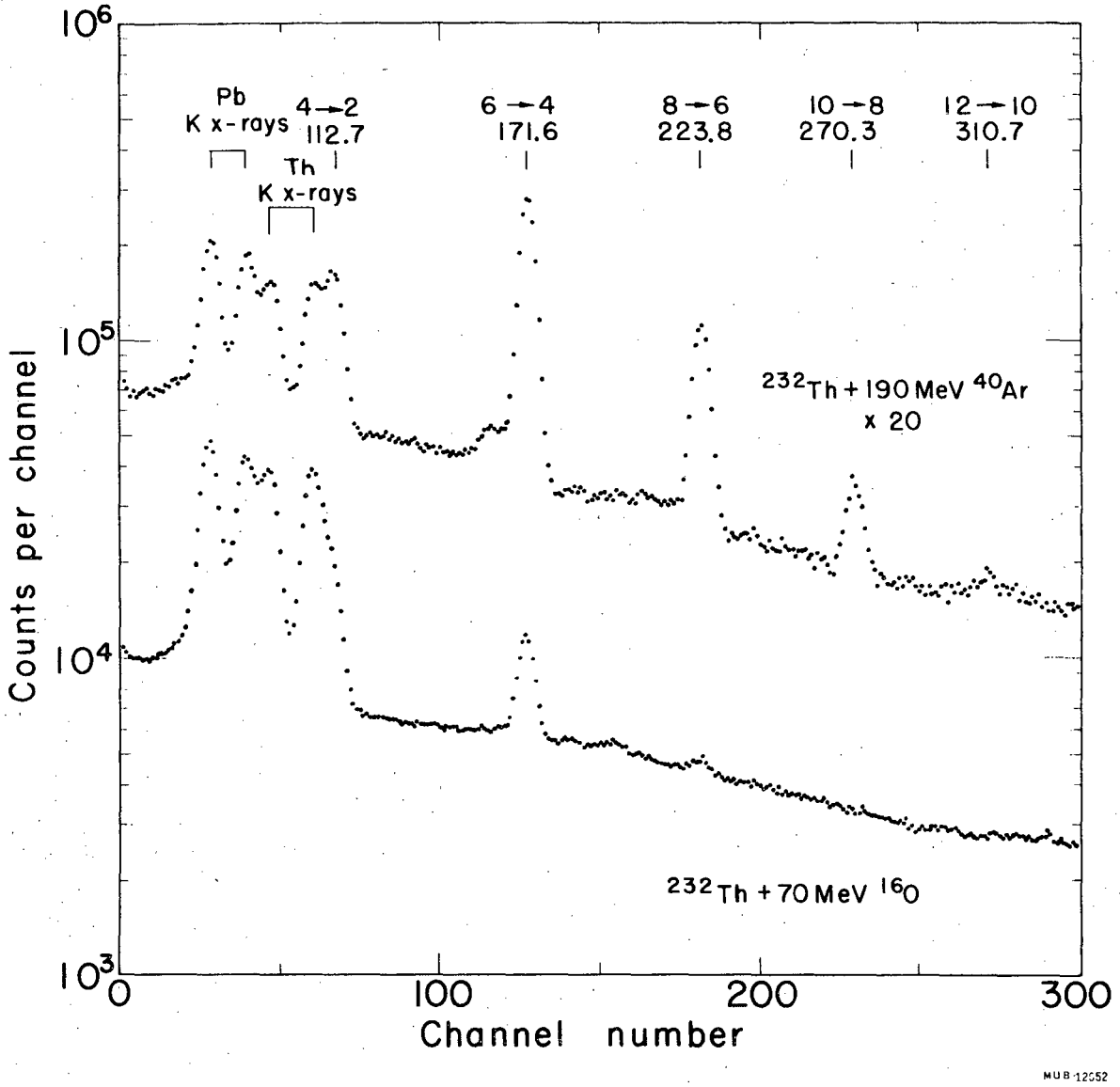
Pb
K x-rays
4→2
112.7
Th
K x-rays
6→4
171.6
8→6
223.8
10→8
270.3
12→10
310.7
232Th + 190 MeV 40Ar
x 20
232Th + 70 MeV 16O
Counts per channel
Channel number
MUB-12052

Fig. 1

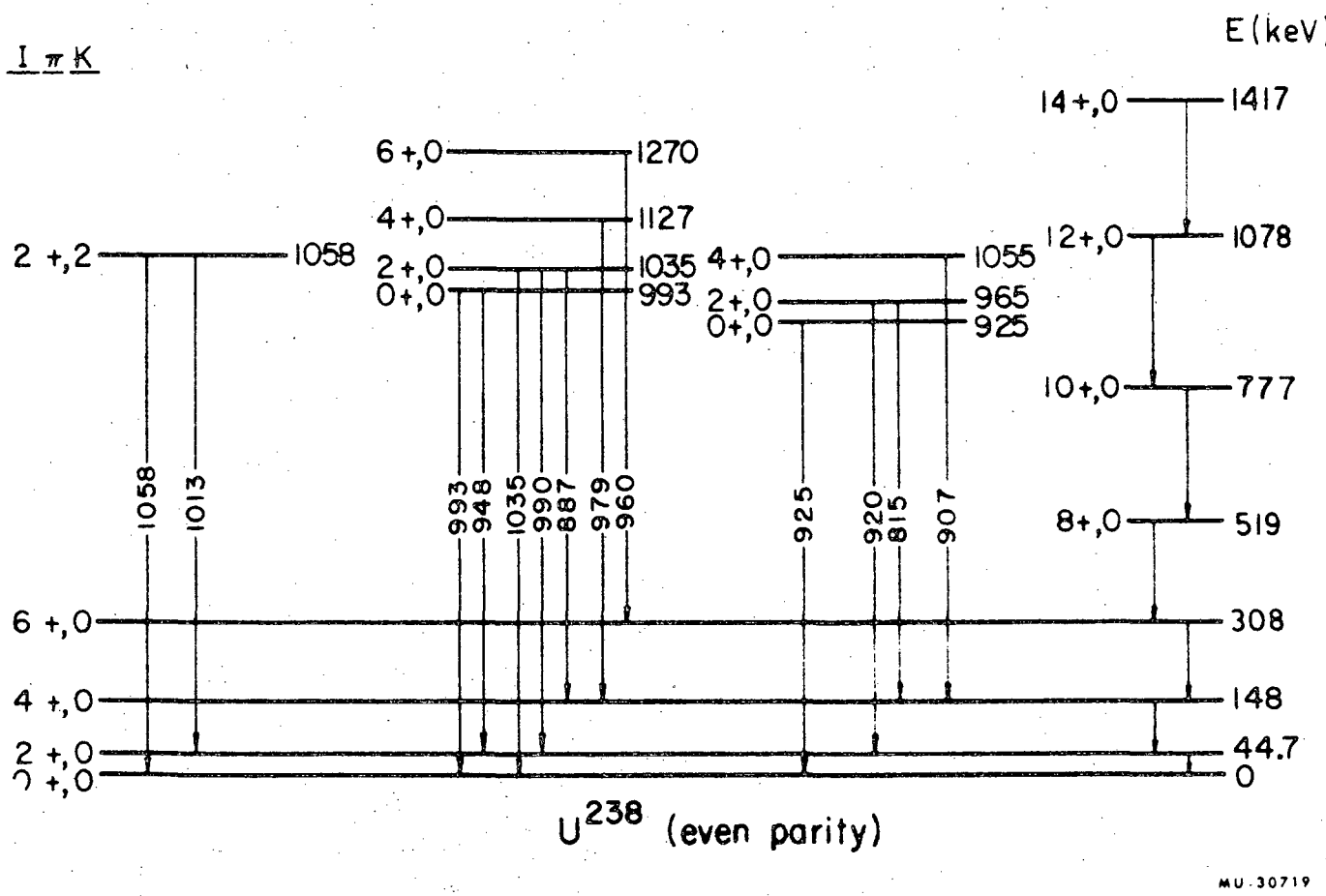
I π K
E(keV)
14+,0
1417
12+,0
1078
10+,0
777
8+,0
519
6+,0
1270
4+,0
1127
2+,2
1058
2+,0
1035
0+,0
993
4+,0
1055
2+,0
965
0+,0
925
1058
1013
993
948
1035
990
887
979
960
925
920
815
907
6+,0
308
4+,0
148
2+,0
44.7
0+,0
0
U238 (even parity)
MU-30719

Fig. 2

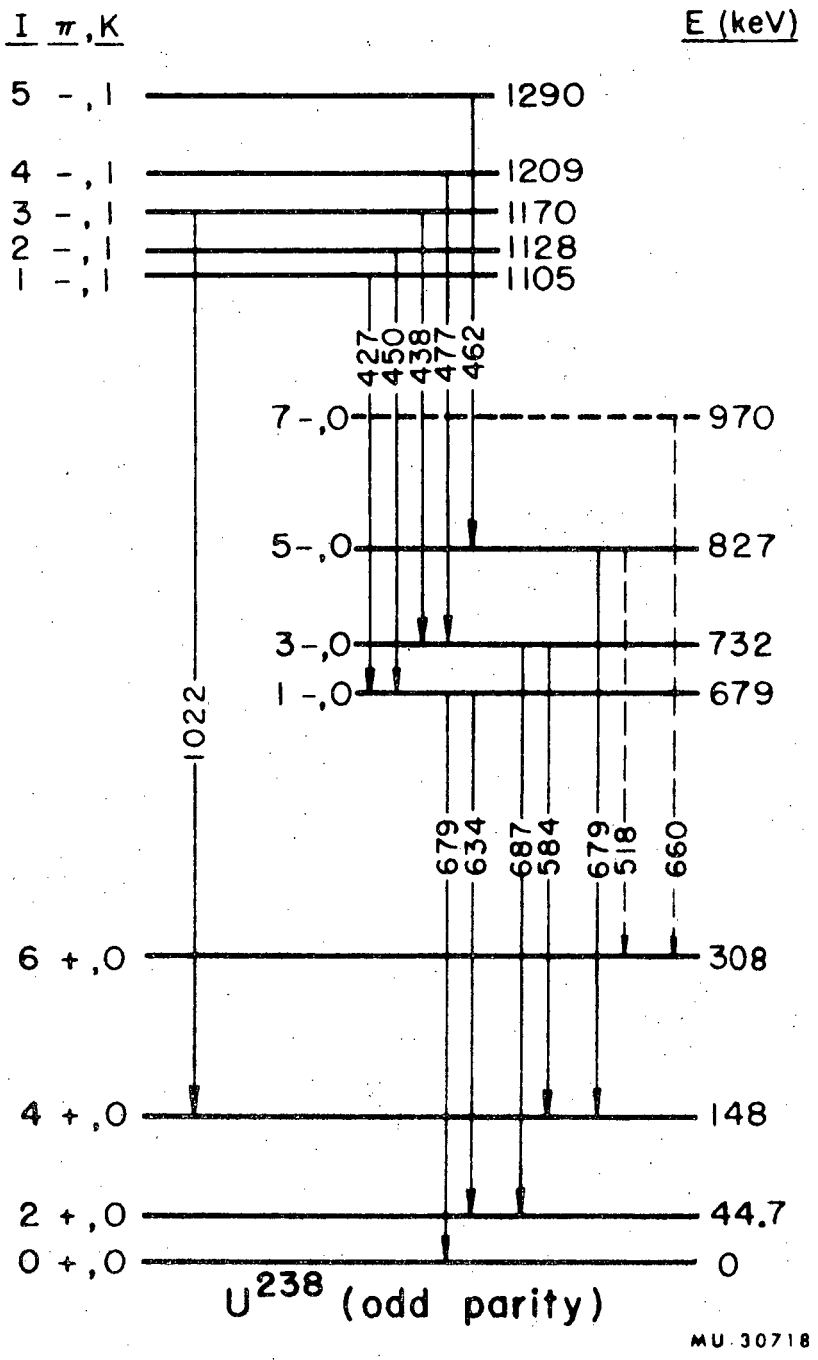
I π,K
E (keV)
5 -,1
1290
4 -,1
1209
3 -,1
1170
2 -,1
1128
1 -,1
1105
427
450
438
477
462
7 -,0
970
5 -,0
827
3 -,0
732
1 -,0
679
1022
679
634
687
584
679
518
660
6 +,0
308
4 +,0
148
2 +,0
44.7
0 +,0
0
U238 (odd parity)
MU-30718

Fig. 3

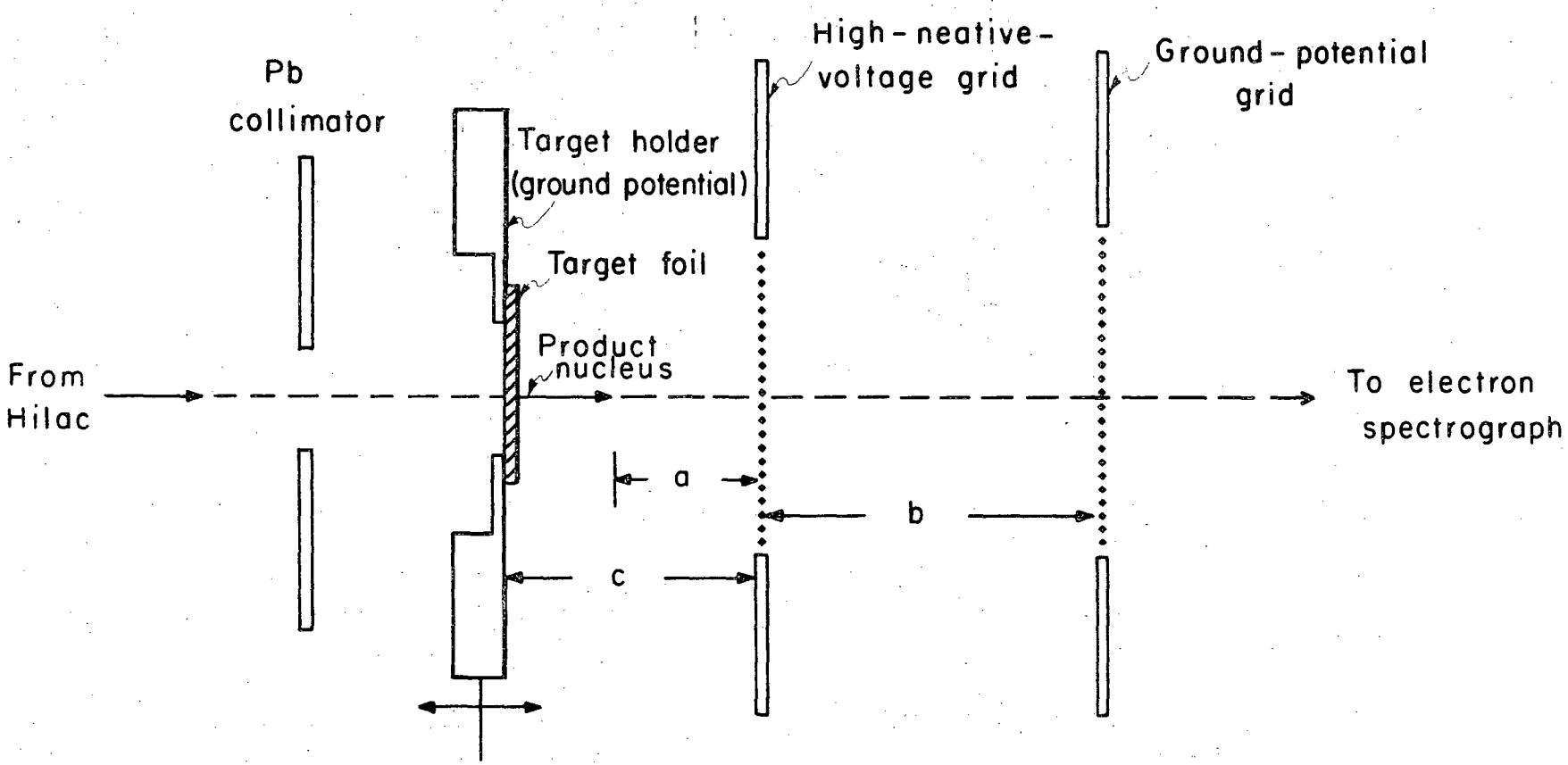

Fig. 4

MU-35634

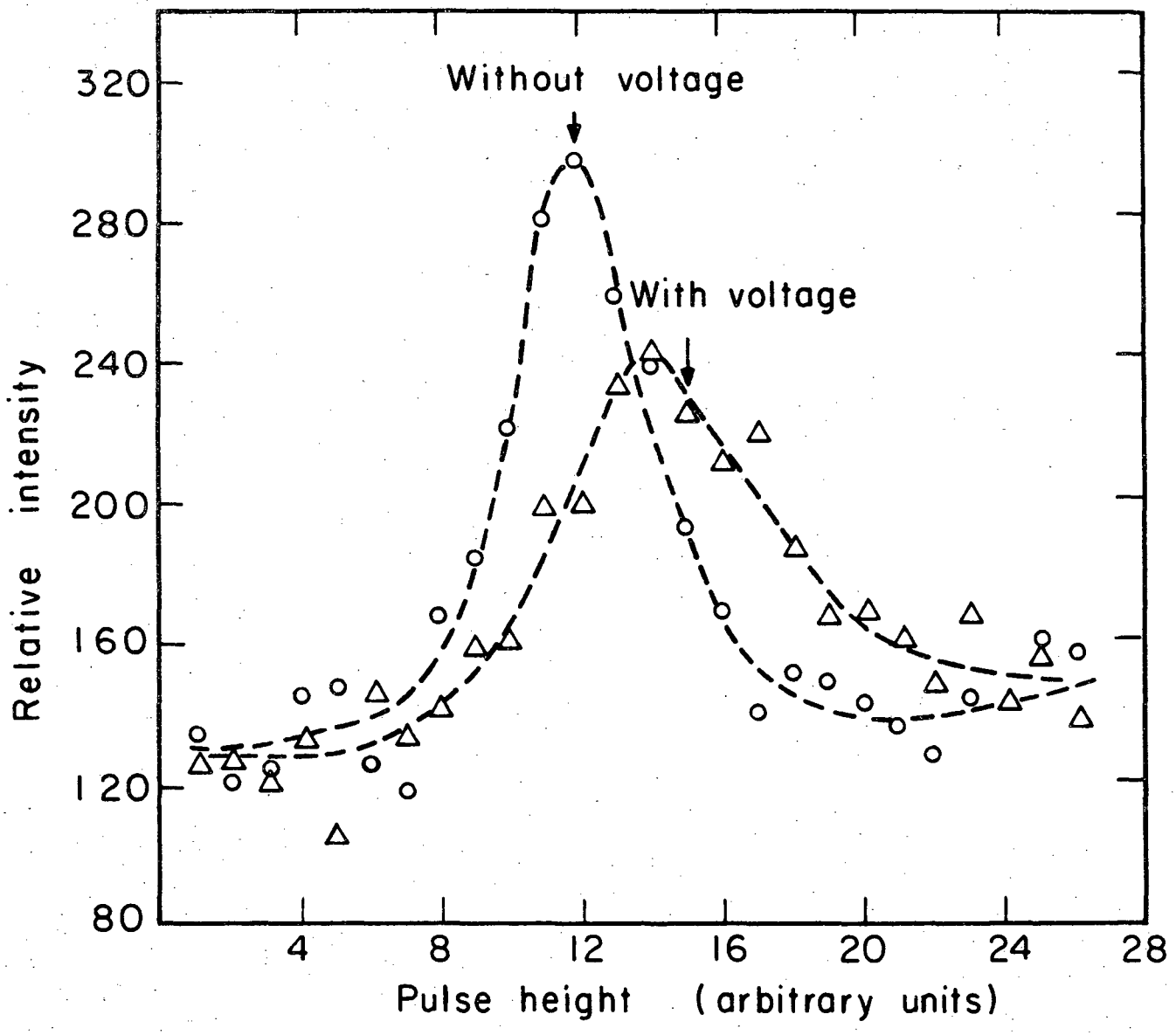

Fig. 5

MU-35628

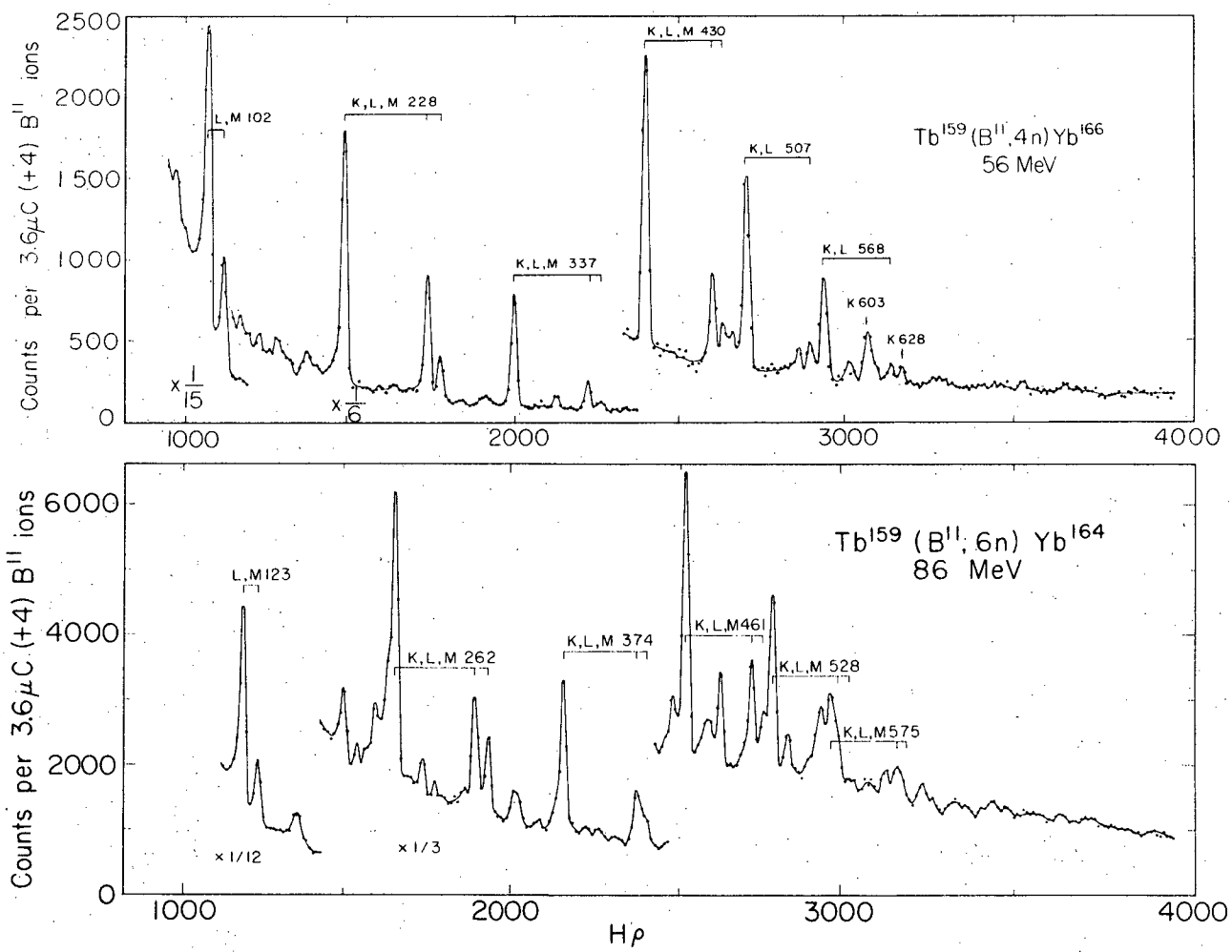

MUB-3674

Fig. 6

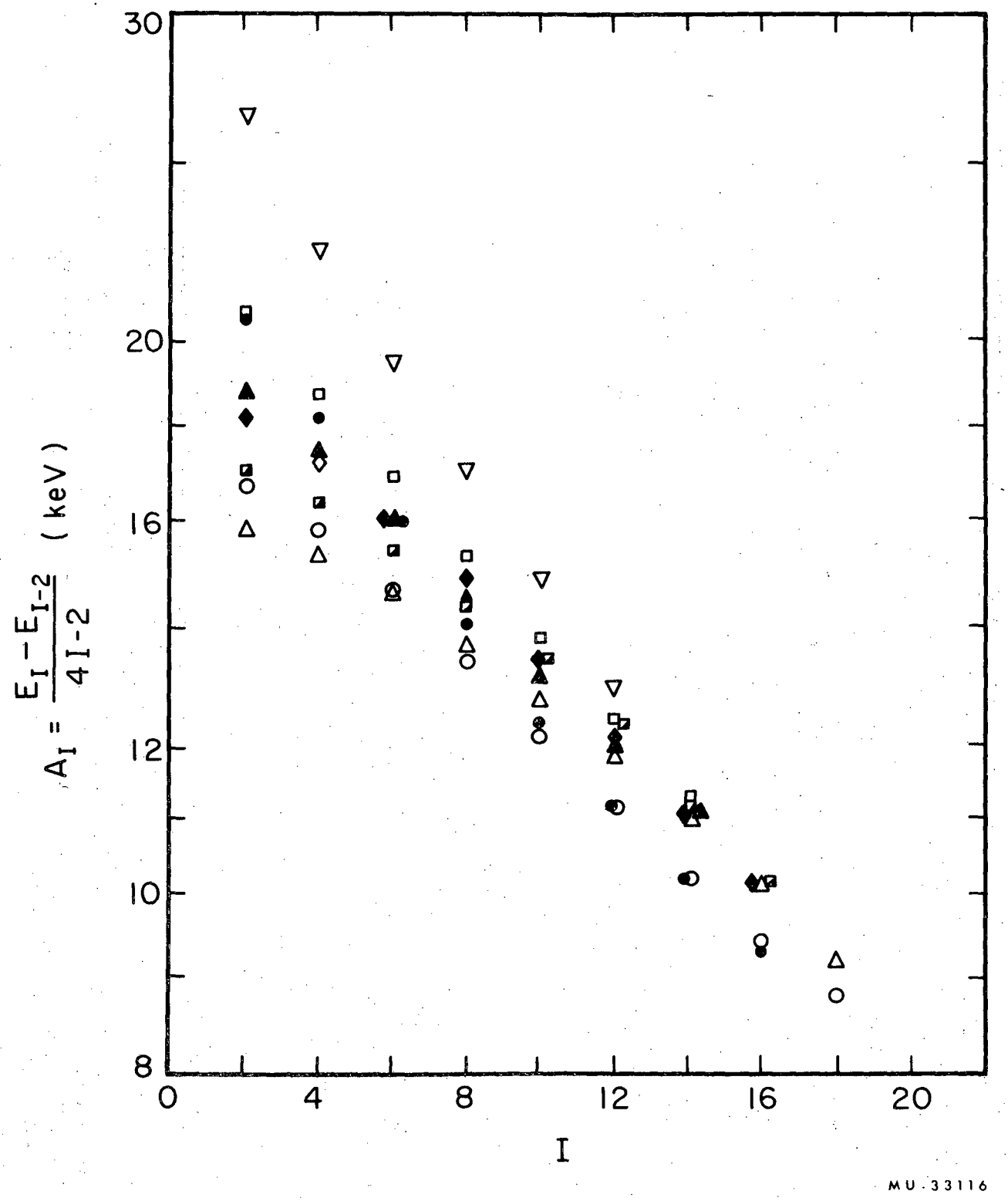

Fig. 7

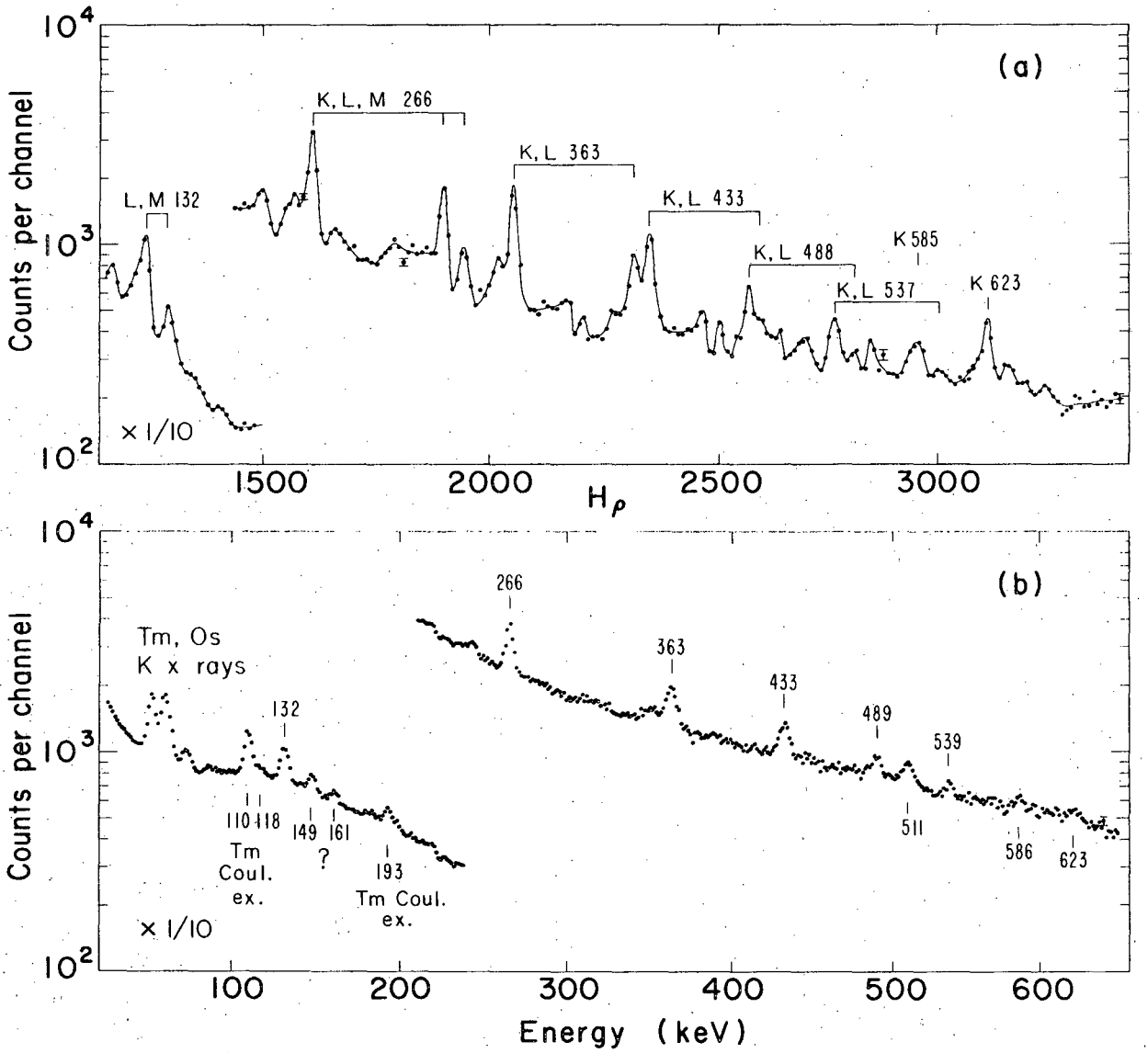
(a)
Counts per channel
10^4
10^3
10^2
K, L, M 266
K, L 363
K, L 433
K, L 488
K, L 537
K 585
K 623
L, M 132
× 1/10
1500
2000
2500
3000
H_ρ
(b)
Tm, Os
K x rays
266
363
433
489
539
511
586
623
132
110 118
149 161
?
193
Tm Coul. ex.
Tm Coul. ex.
× 1/10
100
200
300
400
500
600
Energy (keV)
MUB-10496

Fig. 8

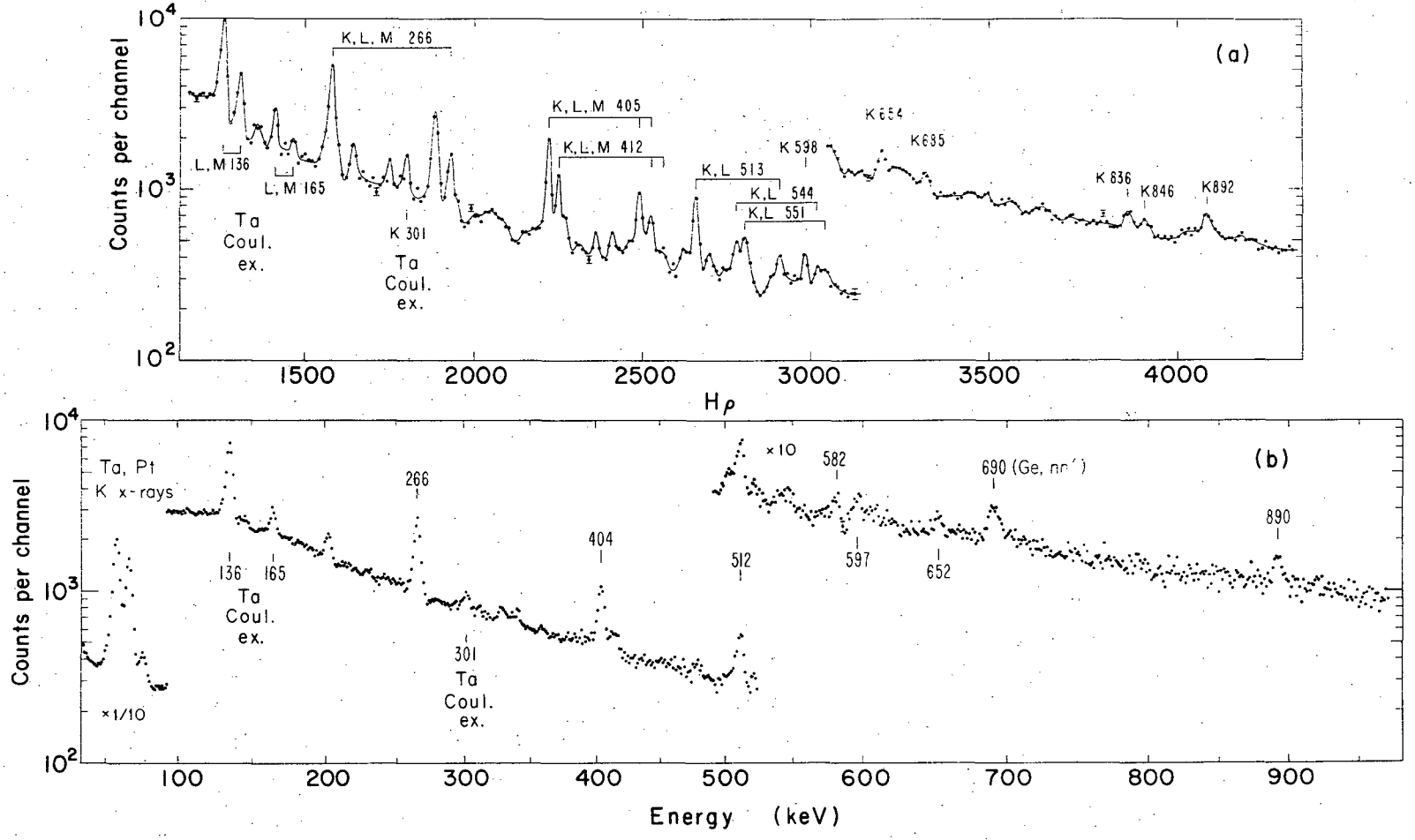
(a)
Counts per channel
10^4
10^3
10^2
K, L, M 266
K, L, M 405
K, L, M 412
K, L 513
K, L 544
K, L 551
K 598
K654
K685
K 836
K846
K892
L, M 136
L, M 165
K 301
Ta Coul. ex.
Ta Coul. ex.
1500
2000
2500
3000
3500
4000
Hρ
(b)
Ta, Pt K x-rays
×1/10
×10
136
165
266
301
404
512
582
597
652
690 (Ge, nn′)
890
Ta Coul. ex.
Ta Coul. ex.
100
200
300
400
500
600
700
800
900
Energy (keV)

Fig. 9

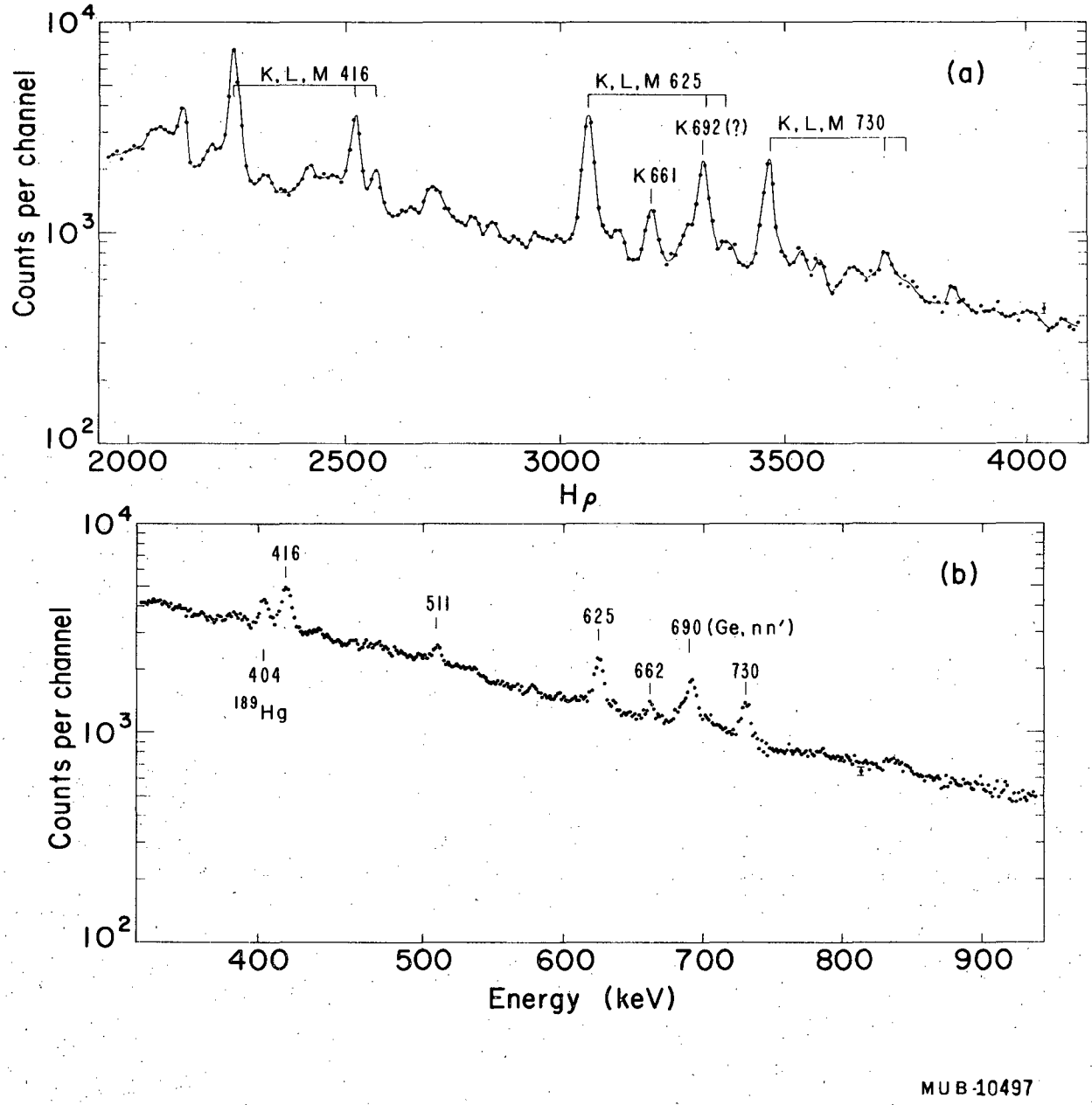
(a)
K, L, M 416
K, L, M 625
K 692 (?)
K, L, M 730
K 661
Counts per channel
Hρ
(b)
416
511
625
690 (Ge, nn')
404
189Hg
662
730
Counts per channel
Energy (keV)
MUB-10497

Fig. 10

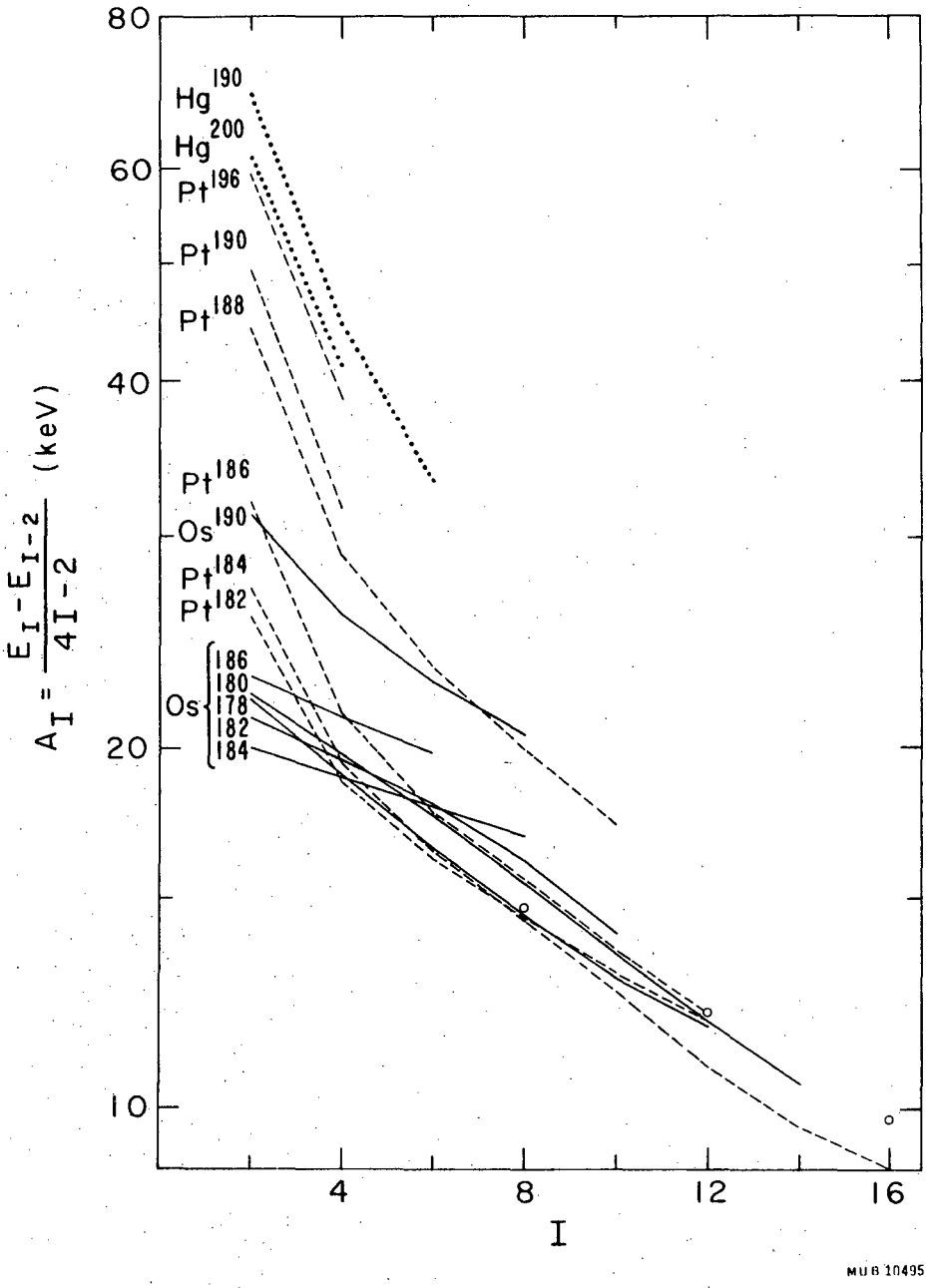
80
60
40
20
10
4
8
12
16
I
$A_I = \frac{E_I - E_{I-2}}{4I-2}$ (keV)
Hg 190
Hg 200
Pt 196
Pt 190
Pt 188
Pt 186
Os 190
Pt 184
Pt 182
Os 186
Os 180
Os 178
Os 182
Os 184
MUB 10495

Fig. 11

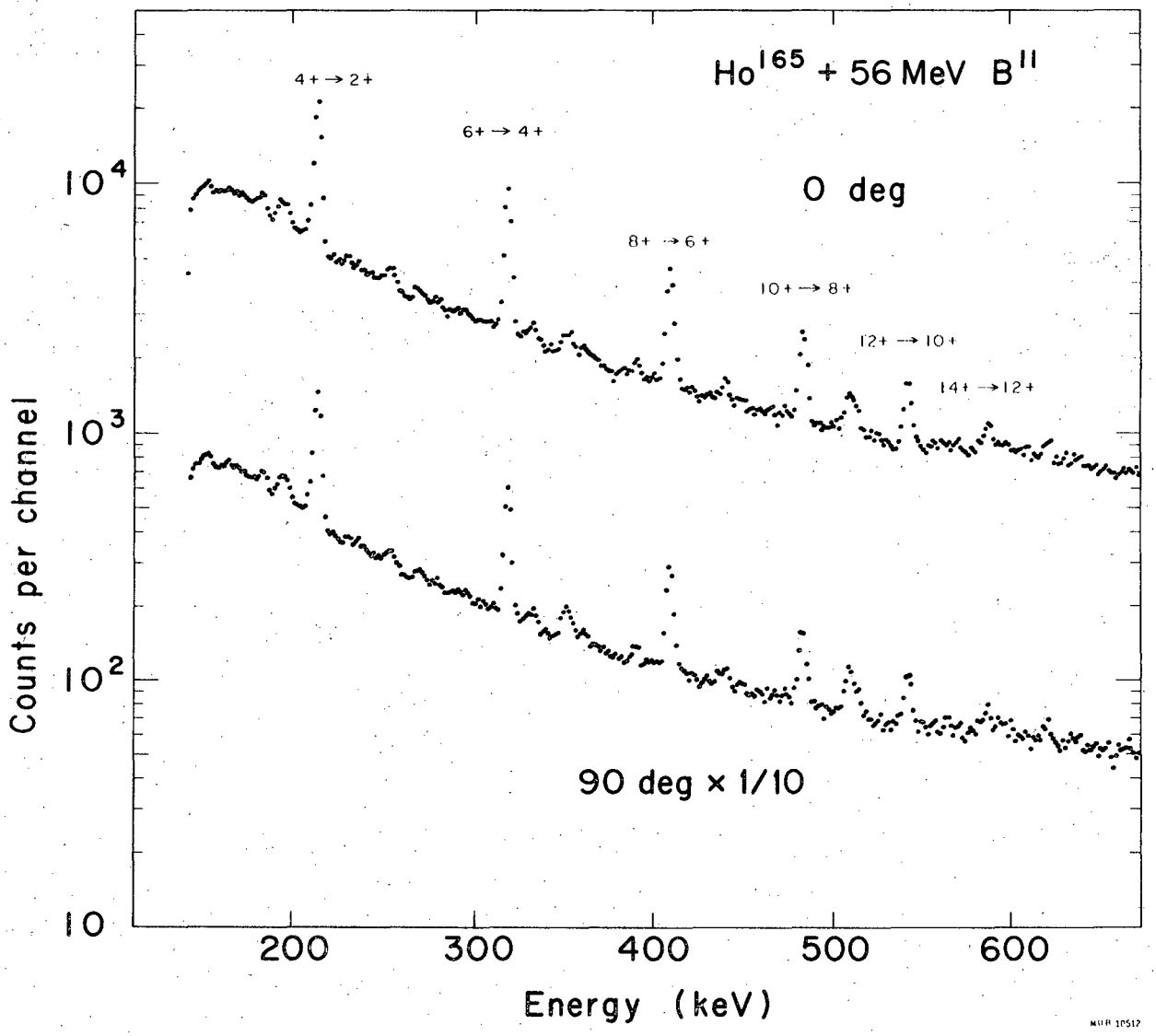
Ho165 + 56 MeV B11
4+ → 2+
6+ → 4+
8+ → 6+
10+ → 8+
12+ → 10+
14+ → 12+
0 deg
90 deg × 1/10
Counts per channel
Energy (keV)
10
10²
10³
10⁴
200
300
400
500
600

Fig. 12

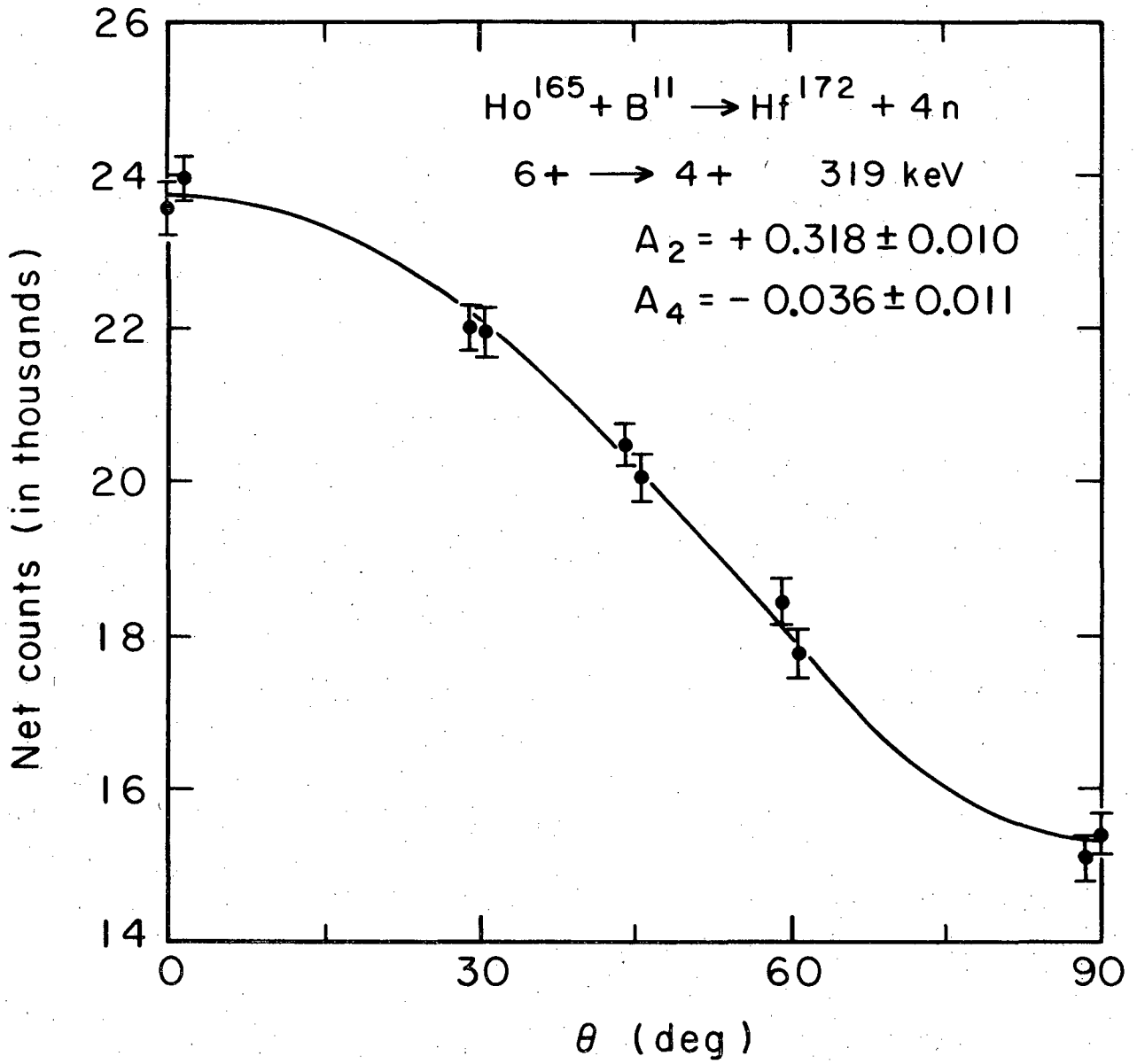

MUB-10509

Fig. 13

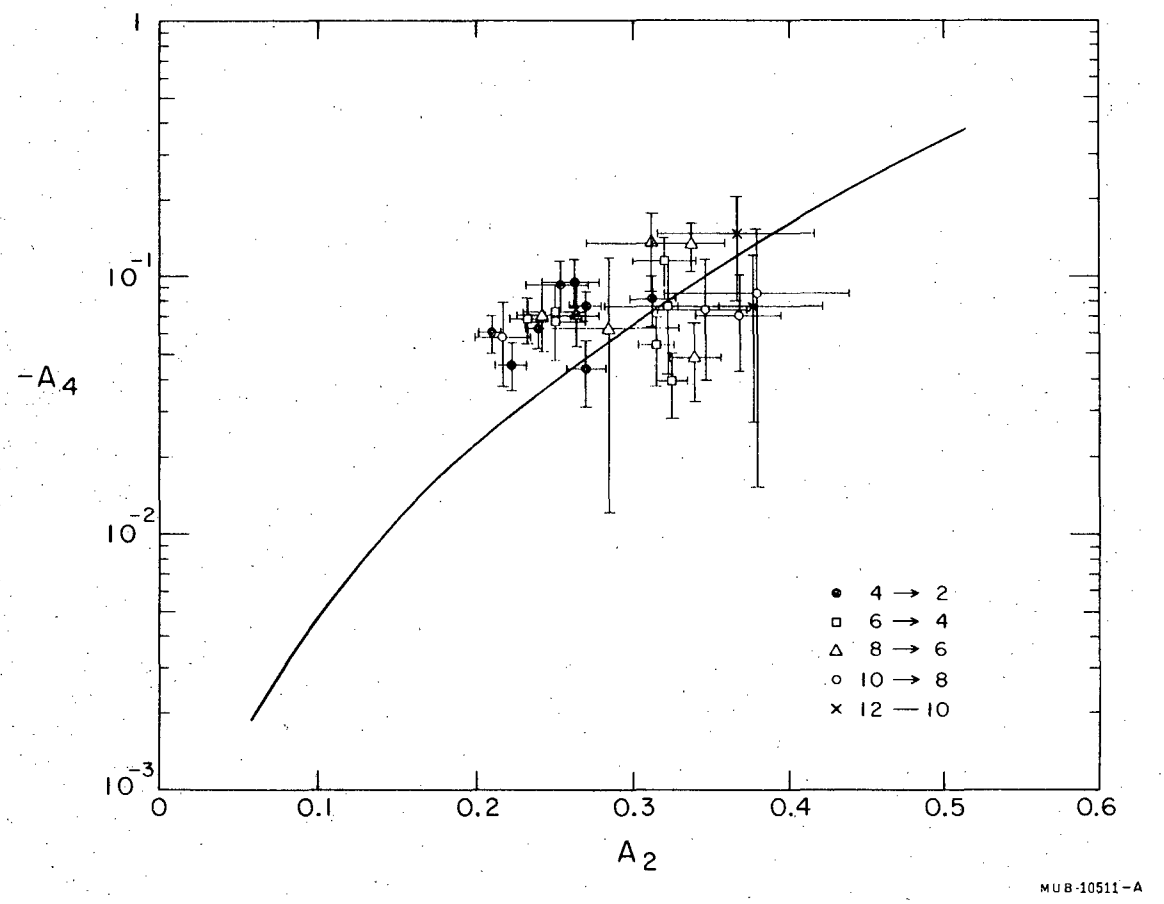

Fig. 14

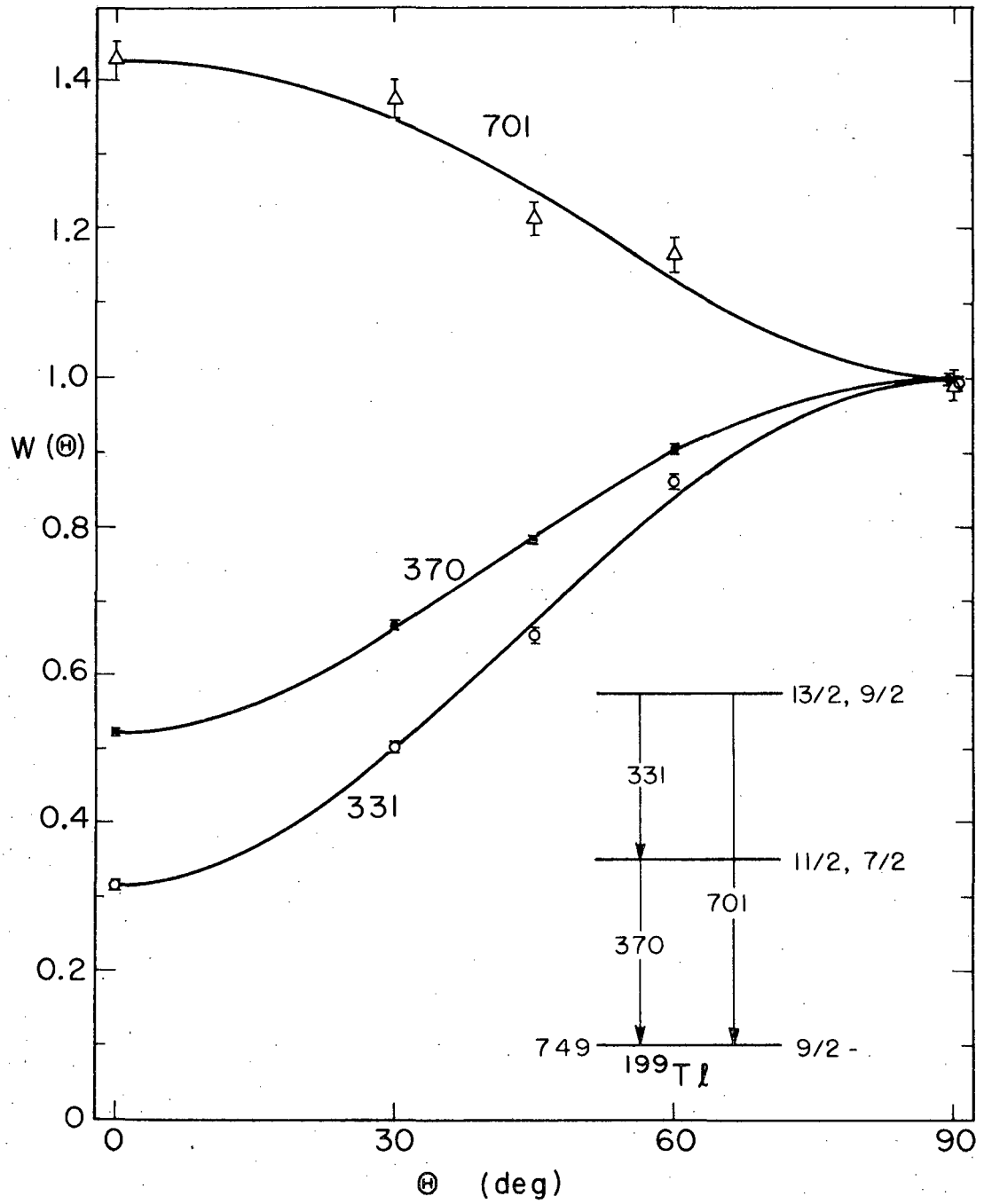
1.4
1.2
1.0
0.8
0.6
0.4
0.2
0
W (Θ)
701
370
331
0
30
60
90
Θ (deg)
13/2, 9/2
331
11/2, 7/2
701
370
749
9/2 -
199Tl
MUB-10867

Fig. 15

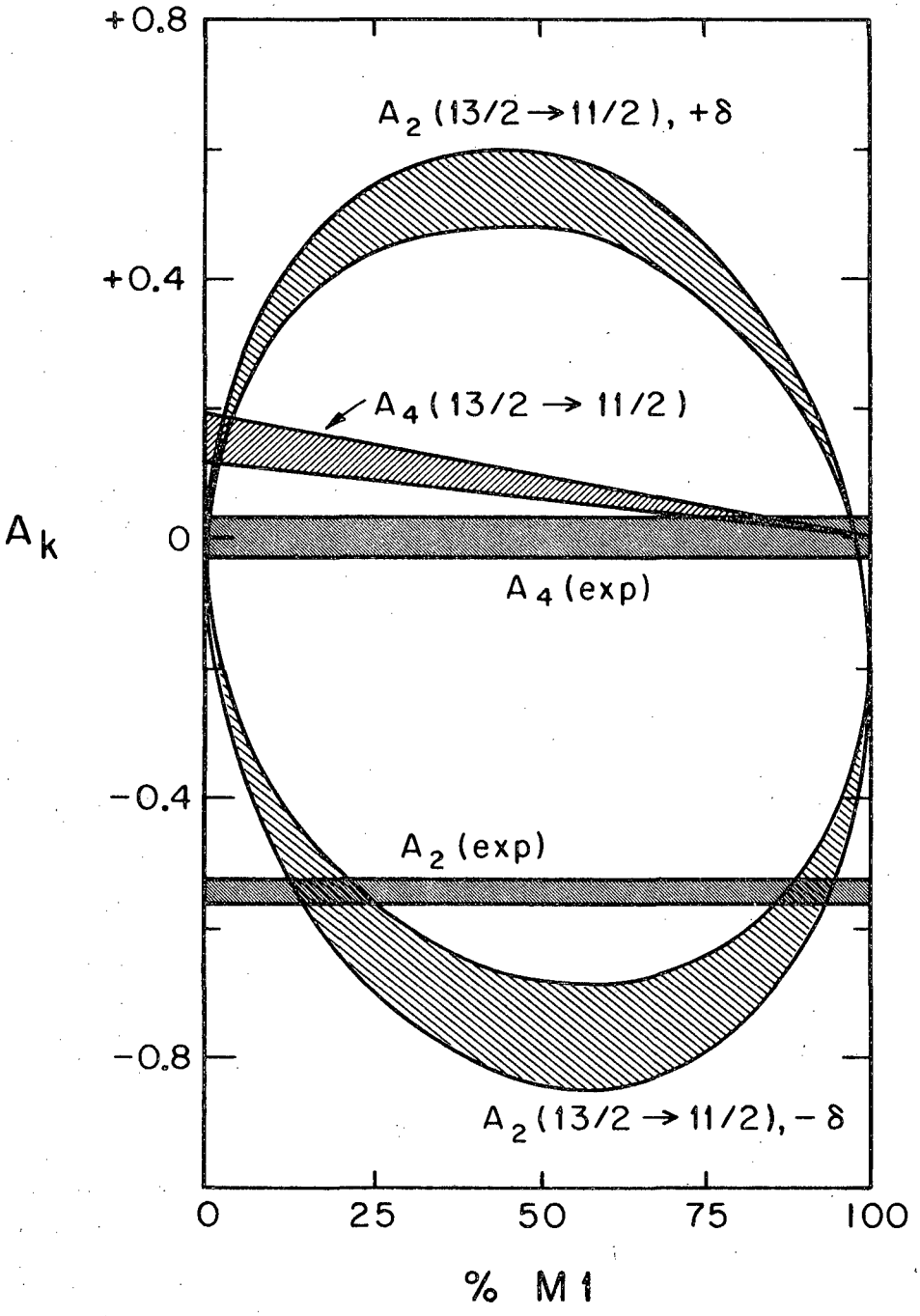
+0.8
+0.4
0
-0.4
-0.8
A_k
A_2 (13/2→11/2), +δ
A_4 (13/2 → 11/2)
A_4 (exp)
A_2 (exp)
A_2 (13/2 → 11/2), − δ
0
25
50
75
100
% M1
MUB-10510

Fig. 16